Size Effect on Strength of Floating Sea Ice under Vertical Line Load

Zdeněk P. Bažant, F.ASCE,[1] and Zaoyang Guo[2]

Abstract: The size effect on the nominal strength of a floating ice plate subjected to a vertical uniform line load is analyzed. The cracks produced by the load, which are parallel to the load line, are treated as softening inelastic hinges. The problem is one dimensional in the direction normal to the load line, equivalent to a beam on elastic foundation provided by buoyancy of ice in water. The softening moment-rotation diagram of inelastic hinges is simplified as linear and its dependence on structure size (ice thickness) is based on the energy dissipated by fracture. For thick enough plates, no two hinges (on one side of the line load) can soften simultaneously, in which case a simple analytical solution is possible. In that case, the load-deflection diagram has multiple peaks and troughs and consists of a sequence of spikes that get progressively sharper as the plate thickness increases. In terms of a dimensionless nominal strength, the effect of a finite fracture process zone at ice surface leads to an up-and-down size effect plot, such that each load peak decreases with the size at first but then asymptotically approaches a rising asymptote of the type $(\text{thickness})^{1/4}$ (which implies a reverse size effect, caused by buoyancy). The energy dissipation when the crack in the hinge gets deep causes a strong monotonic size effect, such that the dimensionless troughs between two spikes, in the case of thick enough plate, decrease asymptotically as $(\text{thickness})^{-1/2}$. For thin enough plates, more than one hinge soften simultaneously and, in the asymptotic case of vanishing ice thickness, the plasticity solution, which has no size effect, is approached. In the intermediate size range with hinges softening simultaneously, the exact solution is complicated and only approximate formulas for the size effect are possible. They are constructed by asymptotic matching.

DOI: 10.1061/(ASCE)0733-9399(2002)128:3(254)

CE Database keywords: Floating ice; Vertical loads; Size effect; Sea water; Strength.

Introduction

When a vertical load is applied over a small area, a floating sea ice plate develops radial bending cracks in a star pattern. This is a two-dimensional problem, for which accurate analytical solutions are not possible. One must either use many approximations of uncertain accuracy (Bažant 2000b; 2001a) or resort to numerical solutions that lack generality and transparency (Bažant and Kim 1998a, b). However, when a floating sea ice plate is subjected to a vertical line load, the ice plate develops bending cracks parallel to the load line. This is a one-dimensional problem, relevant to a railroad or a very elongated building placed on the ice, or to a train of vehicles or sleds, or a file skiers, traveling on the ice. For this problem, an accurate analytical solution is possible and is derived in this paper. Analytical solutions have the advantage that they provide understanding and clarify various influences, especially the size effect, which has recently been the subject of extensive debates (e.g., Bažant, and Kim 2000; Dempsey 2000; Sodhi 2000).

[1]Walter P. Murphy Professor of Civil Engineering and Materials Science, Northwestern Univ., Evanston, IL 60208 (corresponding author). E-mail: z-bazant@northwestern.edu

[2]Graduate Research Assistant, Northwestern Univ., Evanston, IL 60208.

Note. Associate Editor: Arup K. Maji. Discussion open until August 1, 2002. Separate discussions must be submitted for individual papers. To extend the closing date by one month, a written request must be filed with the ASCE Managing Editor. The manuscript for this paper was submitted for review and possible publication on January 5, 2001; approved on August 15, 2001. This paper is part of the ***Journal of Engineering Mechanics***, Vol. 128, No. 3, March 1, 2002. ©ASCE, ISSN 0733-9399/2002/3-254–263/$8.00+$.50 per page.

The bending cracks are part-through cracks and the additional rotations due to cracks may be imagined as rotations in a softening hinge inserted into the crack line. In contrast to plastic hinges considered in plastic limit analysis of beams, frames, and plates, the softening hinges can engender a size effect on the nominal strength of structure. This size is very different from the size effect occurring when the structure fails due to propagation of one dominant crack. Explicit approximate formulas for this kind of size effect have recently been derived using the technique of asymptotic matching (Bažant 2000a) borrowed from fluid mechanics. In this technique, one first obtains the solution for extrapolation to an infinite size and to a vanishing size of the structure, even though such sizes may lie far outside the practical range. Then one ''interpolates'' between these extremes, seeking a smooth formula for the entire size range that matches both asymptotic solutions.

The size effect on the softening moment-rotation diagram of a softening hinge considered here is similar to that used in a parallel study of concrete beam structures (Bažant 2000a). Despite this similarity, it turns out that the elastic foundation provided by buoyancy of ice in water leads to a different size effect on the nominal strength of structure.

Brief Review of Researches on Sea Ice Failure

A comprehensive presentation of the mechanical properties of ice is found in Sanderson's (1988) book, and an exposition of the classical results in the reports of Weeks and Assur (1972) and Weeks and Mellor (1984). The early small-scale laboratory tests of sea ice revealed hardly any notch sensitivity and no fracture mechanics behavior. Accordingly, ice failure has been treated

from early to recent times according to either plasticity theory or elasticity theory with a strength limit (Bernstein 1929; Nevel 1958; Kerr 1975; Sodhi 1995a,b; Kerr 1996; Sodhi 1998).

When size effect was observed in tests (e.g., Butiagin 1966), it was attributed exclusively to the randomness of material strength as captured by Weibull (1939, 1951) theory. This theory is based on a qualitative idea of Mariotte (1686) and on the extreme value statistics of the weakest link model initiated by Tippett (1925) and Peirce (1926), rigorously developed by Fisher and Tippett (1928) and Fréchet (1927), and refined by von Mises (1936), Epstein (1948), Freudenthal and Gumbel (1956), Gumbel (1958), etc., and reviewed by Kittl and Diaz (1988), and Bažant and Planas (1998). The statistical explanation of size effect, however, is dubious because the fracture process zone normally occupies a relatively large zone (except for very thick plates), and because the maximum load is not reached at the initiation of fracture but only after large stable crack growth (for detailed arguments, see Bažant and Planas 1998, Chap. 12). Although there is a statistical component to the mean size effect (see the Appendix), the main explanation must be sought in quasi-brittle fracture mechanics. The deterministic size effect, which is analyzed in this study, cannot be ignored.

As revealed by some recent experiments (Dempsey 1991; DeFranco and Dempsey 1992, 1994; DeFranco et al. 1991), especially Dempsey's in situ tests of record-size specimens (Mulmule et al. 1995; Dempsey et al. 1995; Dempsey et al. 1999a,b), sea ice on a large scale does follow fracture mechanics and on scales larger than about 10 m it is in fact very well characterized by linear elastic fracture mechanics (LEFM). Hence, the size effects of fracture mechanics (Bažant 1984, 1993, 1997; Bažant and Chen 1997; Bažant and Planas 1998; Bažant 1999) must exist. They may be expected to be strong, especially when large cracks grow stably prior to reaching the maximum load. This includes sea ice failure under vertical load, which has been analyzed by fracture mechanics at increasing levels of sophistication; e.g., Slepyan (1990), Bažant (1992a,b), Dempsey et al. (1995), Bažant and Li (1994, 1998), Li and Bažant (1984, 1998), Bažant and Li (1994), Li and Bažant (1994), Bažant and Kim (1998a,b), and Dempsey et al. (1995). Various fine points of the vertical penetration problem and the relevant literature were recently discussed by Dempsey (2000), Sodhi (2001), and Bažant and Kim (2000).

The micromechanics of ice failure in compression, which leads to softening damage, was documented by the studies of Schulson (1990, 2001). The existence of compression softening in ice can also be clearly discerned from the test data reported by Sodhi (1995a,b, 1996, 1998).

Extending previous researches of size effect in sea ice at Northwestern Univ. (Bažant and Kim 1985; Bažant and Gettu 1991; Bažant 1992a,b; Bažant and Li 1994; Li and Bažant 1994; Bažant et al. 1995; Li and Bažant 1998), Bažant and Kim (1998a,b) undertook a detailed large-scale numerical analysis of the size effect in the vertical penetration by a concentrated load (which is imagined, of course, as an approximation to a load actually applied over a small area). The radial cracks emanating from the load were subdivided into many vertical strips in each of which the vertical crack initiation and propagation was modeled by a simplified version of the cohesive crack model. The normal forces in the crack ligaments and the inherent dome effect were taken into account. The elasticity of the floating wedge segments of the ice plate between the adjacent radial cracks was simulated by the variational finite difference method. The analysis confirmed the existence of a strong size effect, approximately following the law proposed by Bažant (1984) (cf. Bažant and Planas 1998). Although the existing field test data on size effect in vertical ice penetration (Frankenstein 1963, 1966; Lichtenberger 1974) are rather scattered and have a limited size range, they nevertheless confirm the existence of size effect and are found not to disagree with the size effect resulting from extensive numerical fracture analysis (Bažant and Kim 1998b).

More detailed recent discussions of previous studies of vertical penetration under a concentrated load are given, for example, in Bažant (2000b), and Bažant and Kim (2000). A fracture mechanics study of the large-scale thermal bending fracture of floating ice (Bažant 1992a,b), which is a related problem, also revealed a strong size effect.

An approximate analytical derivation of the size effect law for the related problem of a concentrated vertical load has recently been presented in Bažant (2000b). The law obtained was shown to agree well with the results of previous large-scale numerical simulations (Bažant and Kim 1998a,b), which were previously found not to be in conflict with the scant field test data found in the literature (Frankenstein 1963, 1966; Lichtenberger et al. 1974).

Deterministic Size Effect on Moment-Rotation Diagram

For homogeneous materials in which the fracture process zone is very small compared to the cross section dimension, the size effect on flexural strength for failures occurring at fracture initiation is governed by Weibull statistical theory of random strength. However, as shown by recent studies, the size effect on flexural strength at fracture initiation in heterogeneous quasi-brittle materials with a sizable fracture process zone is predominantly deterministic (unless the plate is much thicker than the process zone size). It is caused by stress redistribution in the boundary layer of cracking that develops before the maximum load, and the associated energy release (Bažant and Li 1995a,b; 1996; Bažant and Planas 1998, Bažant and Novák 2000a,b; Bažant 2002). Because of the heterogeneous quasi-brittle nature of sea ice, the deterministic theory of size effect on flexural strength will be assumed to hold for sea ice (however, it would not be difficult to include Weibull-type size effect in the present analysis; see the Appendix).

According to a detailed analysis in Bažant (2000a, 2001c), the size effect on the peak bending moment M_p occurring at fracture initiation from the surface of a plate may be approximately described as

$$M_p=\frac{M_\infty}{Q(h)},\quad M_\infty=\frac{\sigma_0 h^2}{6},\quad Q(h)=\frac{h+D_b}{h+2D_b}\quad (\text{all } h)\quad (1)$$

(Fig. 1 top and middle left). Here σ_0 = tensile strength of ice; h = ice plate thickness; D_b = material constant characterizing the thickness of the boundary layer of cracking in sea ice; and function $Q(h)$ characterizes the size effect on flexural strength; $\lim Q(h)=1$ for $h\to\infty$. The thickness D_b is independent of plate thickness and is governed mainly by material heterogeneity; it roughly corresponds to the size of the fracture process zone in vertical fracture of sea ice. For a more detailed justification and discussion of Eq. (1), see Bažant (2000a).

After the boundary layer of cracking fully develops, a vertical crack initiates from this layer (Fig. 1 middle right). The diagram of bending moment M versus the additional relative rotation θ across the hinge plane caused by vertical fracture propagation (Fig. 1 bottom right) may be derived from fracture mechanics

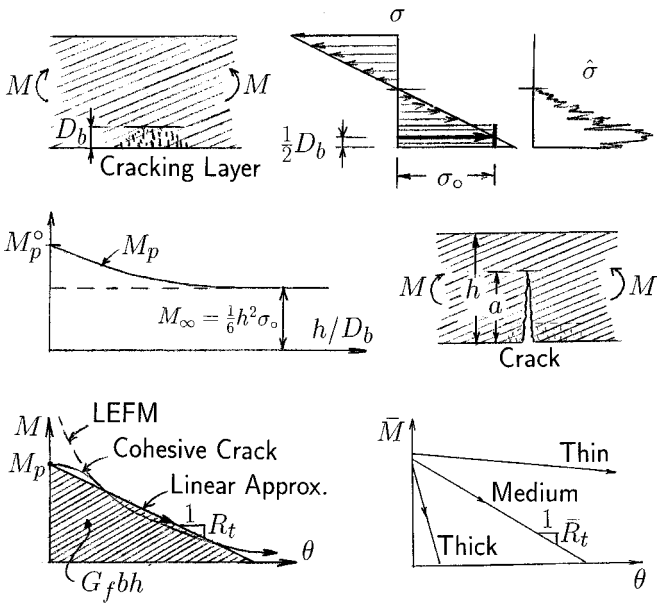

Fig. 1. Top: boundary layer of cracking in a plate, elastic distribution of normal stress σ, and random scatter of microstress $\hat{\sigma}$. Middle: Size effect on flexural strength (modulus of rupture) due to boundary layer of cracking, and softening hinge with a crack. Bottom: Moment-rotation diagram and its dependence on ice thickness h.

(Rice and Levy 1972). According to linear elastic fracture mechanics (LEFM), this diagram starts by a descent from infinity and gradually approaches the horizontal axis. However, because of the finite cohesive zone at the crack front, the softening diagram starts its descent from a finite peak moment, M_p. The descent will be assumed, for the sake of simplicity, to be linear (triangular, Fig. 1 bottom), characterized as

$$\frac{|M|}{M_p}=1-\frac{|\theta|}{\theta_f} \quad \text{if } |\theta|\leq\theta_f; \quad \text{else} \quad M=0 \tag{2}$$

where M_p = peak bending moment and θ_f = rotation at complete fracture (i.e., the rotation at which M is reduced to 0). They are under the complete diagram $M(\theta)$ (Fig. 1 bottom left) must be equal to $G_f h$ (per unit length in the horizontal y direction), G_f being the fracture energy of sea ice. This condition requires that

$$\theta_f=\frac{M_p}{R_t}=\frac{2G_f}{M_\infty}\frac{h}{Q(h)} \tag{3}$$

in which the softening bending stiffness

$$R_t=\frac{M_p^2}{2G_f h}=\frac{M_\infty^2}{2G_f}\frac{1}{q^2(h)h}=\frac{\sigma_0^2}{72G_f}Q^{-2}(h)h^3 \tag{4}$$

If, by contrast, the ice exhibited a fixed (size-independent) softening stress-strain (rather than stress-displacement) diagram, as is the case for plastic materials (e.g., Jirásek and Bažant 2002) and has typically been assumed in earlier studies, R_t would be proportional to h^2 rather than h^3. Therefore, the dimensionless postpeak bending stiffness $\bar{M}/\theta=\bar{R}_t=R_t/Eh^2=M_p/Ebh^2\theta_f$ (where $\bar{M}=M/Ebh^2$ = dimensionless bending moment) is size independent in plasticity. Here, however, it decreases with increasing ice thickness h (Fig. 1 bottom right). This is one source of size effect.

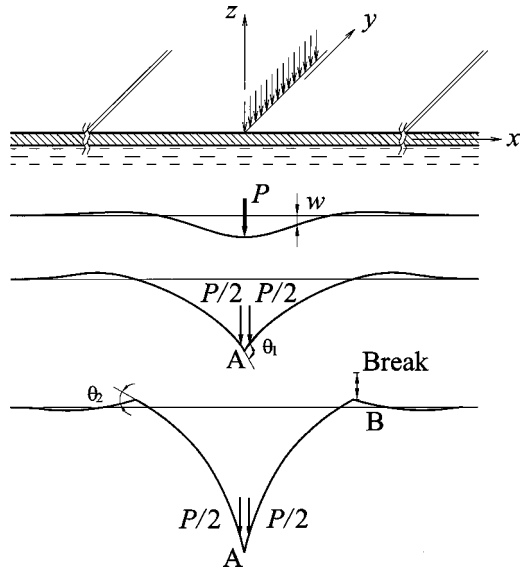

Fig. 2. Floating ice plate subjected to line load, deflection curve, and hinge formation

Mathematical Formulation for Floating Beam with Softening Hinges

A floating plate under a distributed line load (Fig. 2) behaves exactly as a beam on elastic (Winkler) foundation, provided that the top of the plate does not get flooded by water. Such flooding can occur only if the maximum deflection exceeds 9% of ice thickness h, and only if there are cracks and the load duration suffices for water to seep through these cracks. Except for very thin plates, such a deflection is relatively large and large enough seepage cracks are not likely to develop before the maximum load. Therefore, flooding of the top will be assumed not to occur.

The governing differential equation is

$$Dw''''+\rho w=0 \tag{5}$$

where the primes denote derivatives with respect to the length coordinate x; w = plate deflection (Fig. 2), ρ = specific weight of water (force/length^3); $D=E'h^3/12$ = cylindrical stiffness of the plate, $E'=E/(1-\nu^2)$; E is Young's modulus of ice and ν its Poisson ratio. Because of the symmetry of the problem, only the positive branch (including the zero point) needs to be considered. The well-known general solution of this differential equation is

$$w=e^{-\beta x}(C_1\cos\beta x+C_2\sin\beta x)+e^{\beta x}(C_3\cos\beta x+C_4\sin\beta x) \tag{6}$$

where C_1, C_2, C_4, C_4 are constants to be determined from the boundary conditions;

$$\beta=\frac{1}{l\sqrt{2}}=\left(\frac{\rho}{4D}\right)^{1/4}=\left(\frac{3\rho}{E'h^3}\right)^{1/4} \tag{7}$$

and $l=(D/\rho)^{1/4}$ = flexural wavelength (characteristic length) of the floating plate, proportional to the distance between the inflexion points of the deflection curve. The bending moment and shear force are $M=Dw''$, $V=M'=Dw'''$. Eqs. (6) and (7) are valid under the assumption that the in-plane force N normal to the line load is zero or negligible compared to the buckling load (taking N into account, though, would not be much more difficult).

Before the first softening hinge starts to form ($\max M<M_p$), the boundary conditions are $w'=0$ and $V=P/2$ at $x=0$, and w

$=w'=0$ at $x\to\infty$ [Fig. 2(b)]. The latter two conditions require that $C_3=C_4=0$. Setting $M=M_p$ at $x=0$, and denoting the maximum deflection of the plate as $w(0)=w_0$ (which occurs under the load), one obtains the load $P=P_1$ at the start of formation of the first hinge, the corresponding deflection w_0, and the tangential stiffness $K_0=\mathrm{d}P/\mathrm{d}w_0$;

$$P_1=4\beta M_p,\quad w_0=\frac{M_p}{2\beta^2 h},\quad K_0=\frac{P}{w_0}=8\beta^3 h \tag{8}$$

Solution When Ice is Thick Enough for Hinges to Soften in Sequence

Consider now the simple case that the first hinge (that under the load) has fully softened (i.e., $M=0$ at $x=0$) but no other hinge has yet started to form; see Fig. 2(c) (the condition for this to occur will be better discussed in the following section). Now the boundary conditions at $x=0$ change to $w''=0$ and $V=P/2$. The max M occurs at the point where $V=0$ or $w'''=0$; the coordinate of this point is $x=\pi/4\beta$ and

$$\max M=\frac{\sqrt{2}P}{4\beta}e^{-\pi/4} \tag{9}$$

A second hinge (with a symmetric hinge at the opposite side of negative x) starts to form when $\max M=M_p$. This condition yields

$$P=P_2=2\sqrt{2}e^{\pi/4}\beta M_p,\quad w_0=e^{\pi/4}\frac{1}{\sqrt{2}}\frac{M_p}{\beta^2 h},\quad K_1=\frac{P}{w_0}=4\beta^3 h \tag{10}$$

Third, consider again the simple case that the second hinge has also fully softened to $M=0$ [Fig. 2(d)] before another hinge starts to form. Now Eq. (6) can be used only for the segment $x\in(0,\pi/4\beta)$ while, for the rest of the beam up to infinity

$$w=e^{-\beta x}(C_5\cos\beta x+C_6\sin\beta x) \tag{11}$$

The conditions for determining constants $C_1,\ldots,C_6$ are $M=0$, $V=P/2$ at $x=0$, and $M^-=0$, $M^+=0$, $V^-=V^+$, $w^-=w^+$ at the second hinge (superscripts $+$ and $-$ label the values just to the right and just to the left of the point). From this, one can find the stiffness after two hinges (in the right half of the beam) have softened to zero

$$K_2=\frac{P}{w_0}=\frac{e^{\pi/2}-3}{e^{\pi/2}-1}4\beta^3 h=1.901\beta^3 h \tag{12}$$

The load-deflection diagrams for increasing ice thickness h are shown in dimensionless coordinates in Fig. 3. The coordinates are chosen so that the dimensionless load corresponding to P_1 be the same and the initial slope corresponding to K_1 be also the same for all h (in which case the dimensionless slopes corresponding to all K_i are the same as well). This is achieved in Fig. 3 if the coordinate is wh/l^2 and the ordinate is $Pl/[E'h^2Q(h)]$.

Thanks to having assumed a simplified linear moment-rotation diagram for the fracturing hinges, the response diagram of load versus deflection after a hinge starts rotating must also be linear, as shown in the segments from P_1 to P_1' and from P_2 to P_2' in Figs. 3(c–f). The deflection increments for these segments from the start to the end of hinge formation could be calculated by solving again the constants of the general solution of the differential equation with proper interface conditions. However, it is much simpler to exploit the energy balance condition of fracture mechanics.

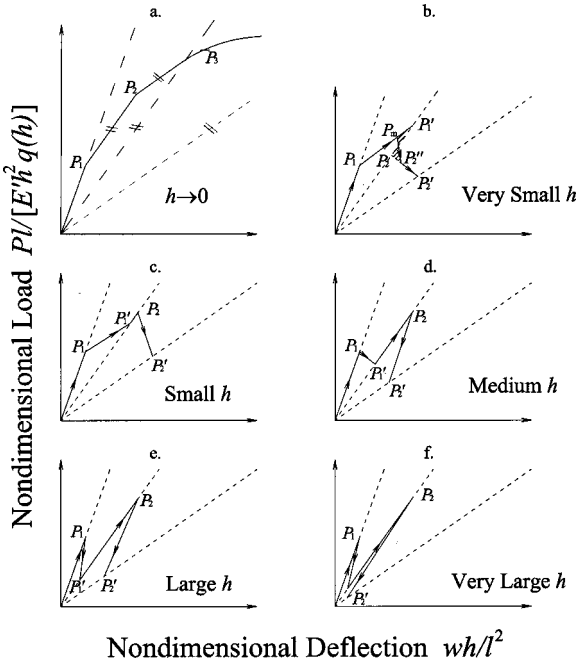

Fig. 3. Diagrams of dimensionless nominal strength versus dimensionless deflection, for increasing values of ice thickness h

First assume that the first hinge has fully softened before the second hinge starts to form [Figs. 3(b–e)]. Then the area W_f of the triangle $0P_1P_1'0$ represents the energy dissipated by the first hinge, which must be equal to the energy needed to create the crack of depth h, which is $G_f h$. Likewise, the area of the triangle $0P_2P_2'0$ must be equal to the energy dissipated by the second hinge in the right half of the beam together with the symmetric hinge in the left half, which is $2G_f h$. The area of each triangle is

$$W_f=\tfrac{1}{2}P_iP_i'(K_i^{-1}-K_{i-1}^{-1}),\quad (i=1,2,3,\ldots) \tag{13}$$

Solving for P_i' and substituting the expressions (8), (10), and (12), one obtains

$$P_1'=\frac{2\beta^2 hM_p}{R_t} \tag{14}$$

$$P_2'=e^{-\pi/4}\sqrt{2}(e^{\pi/2}-3)\frac{\beta^2 hM_p}{R_t}=\frac{1.116\beta^2 hM_p}{R_t} \tag{15}$$

and the corresponding load-point deflections are

$$w_i'=P_i'/K_i \tag{16}$$

The nominal stress of the floating ice plate is a load parameter having the dimension of stress. It is here defined as

$$\sigma_N=P/h \tag{17}$$

where P is the distributed load (of dimension force/length). When P becomes the peak load, σ_N is called the nominal strength. The nominal stresses corresponding to load peaks and troughs P_1,P_1',P_2,P_2' are

$$\frac{\sigma_{N_1}}{\sigma_0 Q(h)}=\frac{P_1}{\sigma_0 Q(h)h}=\left(\frac{16\rho}{27E'}h\right)^{1/4}=\frac{\sqrt{2}}{3}\frac{h}{l} \tag{18}$$

$$\frac{\sigma_{N_1}'}{\sigma_0 Q(h)}=\frac{P_1'}{\sigma_0 Q(h)h}=\frac{G_f}{\sigma_0^2}\sqrt{\frac{12\rho E'}{h}}=\frac{l_f}{l}\frac{h}{l} \tag{19}$$

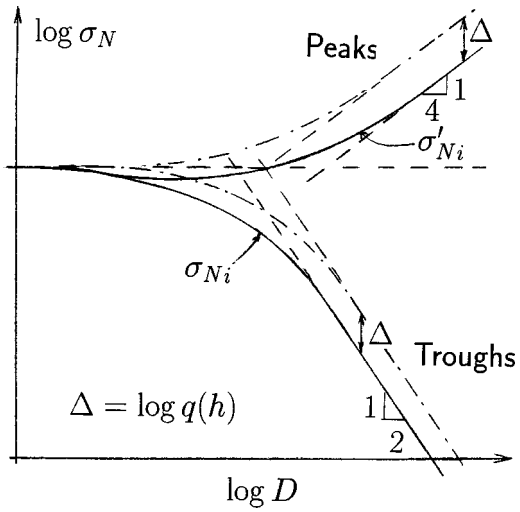

Fig. 4. Logarithmic size effect plots for nominal stresses σ_{N_i} ($i=1,2$) corresponding to the load peaks P_i, and for nominal stresses σ'_{N_i} corresponding to troughs

$$\frac{\sigma_{N_2}}{\sigma_0 Q(h)} = \frac{P_2}{\sigma_0 Q(h) h} = \left(\frac{4e^{\pi}\rho}{27E'}h\right)^{1/4} = \frac{e^{\pi/4}}{3}\frac{h}{l} \tag{20}$$

$$\frac{\sigma'_{N_2}}{\sigma_0 Q(h)} = \frac{P'_2}{\sigma_0 Q(h) h} = \frac{G_f}{\sigma_0^2}\sqrt{\frac{6.696\rho E'}{h}} = 0.7470\frac{l_f}{l}\frac{h}{l} \tag{21}$$

where l represents the flexural wavelength of the plate, and l_f Irwin's characteristic length of the fracture process zone (or material length)

$$l = \left(\frac{D}{\rho}\right)^{1/4} = \left(\frac{E'}{12\rho}\right)^{1/4} h^{3/4}, \quad l_f = \frac{E' G_f}{\sigma_0^2} \tag{22}$$

Note that the scaling of the peaks of the nominal strength ratio $\tilde{\sigma}_N = \sigma_{N_i}/[h\ Q(h)]$ depends only on the ratio h/l and the scaling of the troughs of $\tilde{\sigma}_N$ only on the ratios h/l and l_f/l. The peaks are independent of G_f, but the troughs are not.

The size effect plots, customarily drawn as the plots of the logarithm of these nominal stresses as functions of $\log h$, are shown by the solid curves in Fig. 4 (left). The dashed lines are the asymptotes, and the dash-dot curves are the size effect curves without the effect of $Q(D)$ (i.e., for $Q=1$).

The nominal stresses σ_{N_i} corresponding to the start of each fracturing hinge may either continuously increase (not shown in Fig. 4), which occurs when D_b is large enough, or may first decrease and then increase (shown in Fig. 4), which occurs when D_b is not large enough. The increase of σ_{N_i} represents a reverse size effect, which is caused by the fact that the ratio h/l is not constant but decreases with increasing h (it decreases as $h^{-1/4}$).

The nominal stresses corresponding to the completion of each fracturing hinge decrease as $1/\sqrt{h}$ [after $Q(h)$ approaches a constant value], i.e., they exhibit the standard LEFM-type size effect [Fig. 4(b)]. The consequence is that, with increasing h, the load-deflection slope from P_1 to P'_1 decreases. This slope depends on parameter

$$\kappa = \beta h/R_t = \frac{6E' G_f}{\sigma_0^2}\left(\frac{3\rho}{E'}\right)^{1/4} h^{-3/4} Q^2(h) \tag{23}$$

For $\kappa=2$, the slope is zero (horizontal segment). For $1<\kappa<2$, the slope is negative (softening), which represents an unstable response if the load is controlled. For $\kappa=1$, the slope is vertical, and for $\kappa<1$ the slope changes from negative to positive, which is called the snapback, a behavior that is unstable for both load control and displacement control at the loading point.

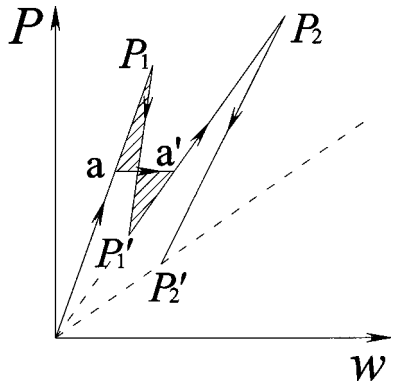

Fig. 5. Maxwell line aa' of possible snapthrough due to imperfections or dynamic disturbances

Whether or not the case of hinges softening one at a time can actually occur for real thicknesses of sea ice in the Arctic is irrelevant. As will be seen, the purpose is to obtain asymptotic support for an asymptotic matching formula valid through the entire range.

Implications for Size Dependence of Imperfection Sensitivity

As thickness h is increased further, the load-displacement diagrams develop sharper and sharper spikes, as seen from the progression of diagrams in Fig. 3. In the limit $h\to\infty$, the spikes become infinitely narrow [Fig. 3(e)]. This limiting behavior is similar to that encountered in shells.

By analogy with shells, the snapback on the load-deflection diagram must be expected to lead to extreme sensitivity to geometric imperfections and dynamic disturbances. This may lead to the so-called snapthrough (e.g., Bažant and Cedolin 1991), illustrated by the horizontal line on the load-deflection diagram in Fig. 5. The cross-hatched triangle above that line represents the kinetic energy of the disturbance required to produce the snapthrough. The line for which the cross-hatched triangle above and below the horizontal line has equal areas is called the Maxwell line (known from the theory of phase changes); for that line the net energy change on passing from point a to point a' is zero.

In the case of snapback, it would be dangerous to take the design load P_1 divided by the usual safety factor. A safe design load must in that case be based on a much reduced load, same as for axially compressed cylindrical shells. So, for large sizes h, the design load exhibits a much stronger size effect than the peaks of the load deflection diagram.

Load-Deflection Behavior When Hinges Soften Simultaneously

So far, we have obtained analytical expressions for the load-deflection diagrams [Figs. 3(c–f)] only for the case that the hinges are not softening simultaneously. From the solution we can see that the hypothesis of the hinges not softening simultaneously is always valid if the plate is sufficiently thick. Vice versa, if the plate is sufficiently thin, the hinges will be softening simultaneously. Let us now discuss such behavior.

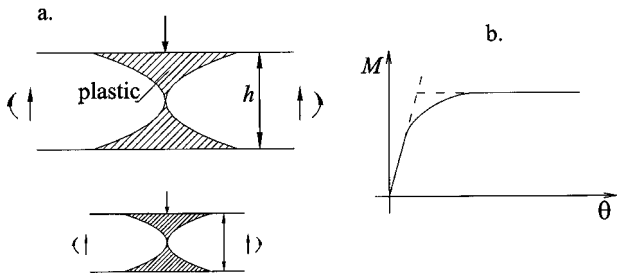

Fig. 6. Yielding zones of plastic hinges for different sizes h, moment-rotation diagram of plastic hinge, and load-deflection diagram of floating ice plate with no flooding on top (note the nonzero terminal slope)

For small enough sizes h, parameter κ becomes higher than 2. Then the load-deflection diagram after P_2 rises [Fig. 3(a)], i.e., the structure exhibits no softening. For $\kappa=3.1$, load P_1' at the first hinge completion becomes equal to load P_2 at the second hinge initiation.

When $\kappa>3.1$, the second hinge begins to form before the first hinge has softened fully, which means that, for a while, both hinges are softening simultaneously. In that case, the boundary condition $w''(0)=0$ does not hold because $M(0)\neq 0$ when the second hinge starts to form, which means the first hinge is not fully softened. Then this condition cannot be used to solve P_2. The preceding simple analysis based on triangular areas $G_f h$ and $2G_f h$ also breaks down.

Fig. 3(a) shows only the case in which the third hinge does not form until the first hinge and second hinge are fully softened. In fact, the third hinge could initiate even before the first hinge is fully softened. Fortunately, in practical cases, parameter κ will not be larger than 3.1. Using the values $E=1.0$ GPa$=1\times10^9$ N/m^2, $\nu=0.29$, $\sigma_0=0.2$ MPa$=2\times10^5$ N/m^2, $\rho=9.81\times10^3$ N/m^3 and $G_f=10$ N/m, typical for sea ice, one can get

$$\kappa=0.118h^{-3/4}Q^2(h) \tag{24}$$

For $\kappa=0.1-6m$, κ will be less than 3.1 because $Q(h)$ is always less than 1. Therefore, the case $\kappa>3.1$ will not be discussed further.

It should, nevertheless, be noted that the case of a plastic hinge, for which the moment-rotation diagrams end with a horizontal plateau, coincides with the asymptotic case $\kappa\to\infty$, which is discussed next.

Load Capacity and Ductility

Once the second hinge has softened to zero, there is a crack all across the thickness. So the shear capacity must drop to zero and the opposite sides of the plate become disconnected, i.e., the opposite faces of the crack can slide vertically. Consequently, the load must immediately drop, as shown in the figure. Thus it makes no sense to look for further hinges to form. The completion of the second hinge obviously represents the ductility limit, i.e., the stability limit under load-point displacement control.

This kind of ductility limit does not occur in plasticity, where the cross section retains a finite shear capacity even at the plastic moment. The plastic limit load is in this case unbounded—as sketched in Fig. 6. The plasticity solution for the present problem, in theory, never reaches a horizontal plateau, as long as the diagram of buoyancy pressure of water versus the deflection remains linear (the same must of course apply to the plasticity solution for the case of concentrated load).

The linear relation between buoyancy force and deflection ceases to hold if there are cracks through which water can seep and flood the top of the plate. The flooding, which can occur (in view of the mass density of ice) only if the deflection exceeds 9% of the plate thickness (a rather large deflection), is mathematically equivalent to plasticization of the foundation (i.e., the buoyancy pressure becomes a constant, independent of deflection). In that case, the plastic solution does reach a horizontal plateau (corresponding to a limit load), but only if the deflection exceeds 9% of ice thickness.

Plastic Hinge Behavior in Asymptotic Case of Vanishing Thickness

If the thickness of the floating ice, h becomes infinitely small, Eqs. (3) and (4) indicate that R_t will also become infinitely small and θ_f will become infinitely large. Then the bending moment magnitude at the hinge will remain M_p, i.e., the hinge will not soften. So the hinge actually behaves as a plastic hinge.

Since the behavior of the hinge will not influence the governing differential equation (5), the general solution of the plate deflection will remain to be Eq. (6). The first part of the load-deflection diagram prior to the formation of the first hinge is the same as in the softening case, and so Eq. (8) can be used to calculate P_1 and the corresponding w_0 and K_0.

Because the first hinge, after it forms, will not get softened, the boundary conditions will be $M=-M_p$, $V=P/2$ at $x=0$, and C_3 and C_4 will remain zero. Now it is found that the max M occurs at the point where $V=0$ or $w'''=0$. The maximum magnitude of M and the coordinate of the point where it occurs are as follows:

$$\max M=M_p\sqrt{2(k^2-4k+8)}\exp\left[\operatorname{arccot}\left(\frac{k-4}{k}\right)\right],$$

$$x=\frac{1}{\beta}\operatorname{arccot}\left(\frac{k-4}{k}\right),\quad k=\frac{P}{\beta M_p} \tag{25}$$

A second hinge (with a symmetric hinge at the negative side of x) starts to form when $\max|M|=M_p$. This condition yields

$$P=P_2=9.7352\beta M_p,\quad x=x_0=\frac{1.0384}{\beta},\quad w_0=1.9338\frac{M_p}{\beta^2 h} \tag{26}$$

As before, after the second hinge forms, Eq. (6) can be used only for the segment $x\in(0,\pi/4\beta)$, while the branch at the right side of the second hinge can be represented as Eq. (11). The boundary conditions must be analyzed carefully. At point $x=0$, one has $M=-M_p$ and $V=P/2$. At the second hinge point $x=x_0$, clearly $M^-=M_p$, $M^+=M_p$, and $V^-=V^+$.

Since the moment at $x=x_0$ is the moment of maximum magnitude possible and the shear force V is proportional to the slope of the bending moment diagram, one finds that $V^-\geqslant 0$ and $V^+\leqslant 0$ at the second hinge. This will cause that $V^-=0$ and $V^+=0$ at the second hinge. C_5 and C_6 can be determined from the values M^+ and V^+, and so they will remain constant even if P is increased.

This means that the deflections w will not change in the beam segment lying beyond the second hinge. Thus, $w^+(x_0)$ will remain equal to $M_p/(2\beta^2 D)$. At the same time, C_1, C_2, C_3, and C_4 can be determined from the values of $M(0)$, $V(0)$, $M^-(x_0)$,

and $V^-(x_0)$. Since $V(0)$ is related to P, one finds that $w^-(x_0)$ will decrease when P is increased above the value $P_2 = 9.7352\beta M_p$. Because $w^+(x_0)$ remains unchanged, deflection w will, therefore, be discontinuous at the second hinge if P is increased above P_2. Since the deflection cannot rise further when the deflection curve is discontinuous, it follows that P_2 must be the maximum load.

To continue the analysis, assume now that w can become discontinuous at the second hinge, while at the same time the beam cannot resist moment M_p. With this assumption, P can be increased above P_2. However, the bending moment within the segment $(0,x_0)$ will reach M_p if P is large enough. Since $V^-(x_0)$ remains zero, the third hinge must be located infinitely close to the second hinge.

In other words, the second hinge will cease to be a point. A plasticized segment will spread to the left (towards the origin of x). The critical point of P, denoted as P_3, is at the point where $w''''(x_0)=0$ because after that the bending moment of maximum magnitude within the segment would exceed M_p. According to the governing equations, this means that $w(x_0)=0$ and it follows that:

$$P = P_3 = 11.038\beta M_p, \quad w_0 = 2.9618\frac{M_p}{\beta^2 h} \tag{27}$$

If P is increased above P_3, the second hinge will get extended leftwards (towards the origin of x). Using x_1 to ascertain the location of the left end of the plastic segment, one finds that the boundary conditions include $M=-M_p$, $V=P/2$ at point $x=0$, and $M=M_p$; $V=0$ and $w=0$ at point $x=x_1$. From these five boundary conditions, the values of C_1, C_2, C_3, C_4, and P can be solved directly. The resulting load-deflection diagram is as shown in Fig. 3(a).

Asymptotic Matching Formulas for Entire Size Range

Our analysis has so far dealt with only with the asymptotic cases, that is, with (1) the case of vanishing ice thickness h for which the plastic limit analysis holds, and (2) the case of sufficiently thick ice for which the hinges do not soften simultaneously. To obtain a general formula for size effect, we now invoke the technique of asymptotic matching:

This technique seeks to obtain an approximate formula for the entire size range, including the intermediate size range which is much harder to solve, by finding a smooth formula that matches these two asymptotic solutions for $h\to 0$ and for $h\to\infty$. Invented by Prandtl about a century ago and exemplified by the boundary layer theory, this technique has been used widely and very successfully in fluid mechanics to interpolate between different asymptotic solutions of differential equations in the spatial coordinate (Bender and Orszag 1978; Barenblatt 1979; Hinch 1991, Sedov 1959). Here, instead of applying this technique in the spatial coordinate x, we do so in size h as the coordinate, which is in fact much simpler.

The size effect formulas (18) and (20) for the peaks and troughs apply only to large enough h for which P_i are peaks and the hinges do not soften simultaneously. For smaller sizes, simple exact formulas cannot be obtained.

However, for $h\to 0$, the solution provided by plasticity is also simple. In similarity to the approach taken for concrete beams and frames (Bažant 2000a), one may exploit the fact that the dependence of nominal strength on h ought to be smooth. For this reason, an approximate formula for the size effect can be obtained by interpolation between the simple size effects for small and large sizes, properly regarded as asymptotic matching in the log h scale. It may be checked that the following smooth approximate formulas for the entire size range have the correct large and small size asymptotic behaviors:

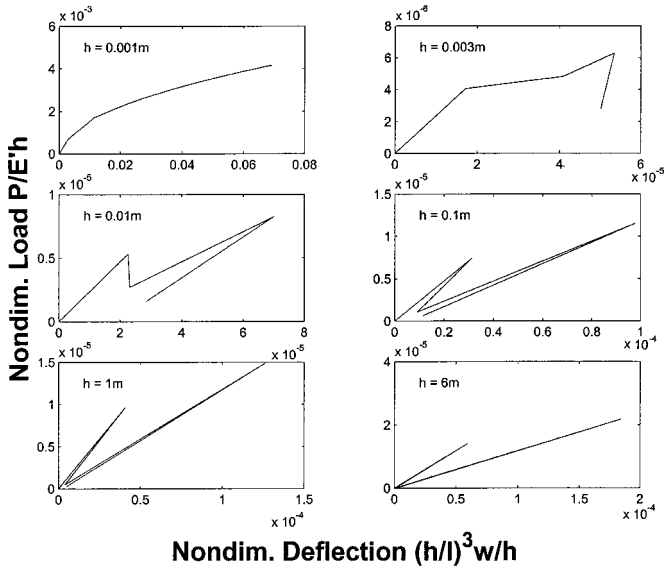

Fig. 7. Numerical example of load-deflection curves calculated for typical ice properties (note that scales in each plot are different)

$$\sigma_{N_1} = \sigma^0_{N_1} Q(h)\left[1+\left(\frac{\sqrt{2}h}{3l}\right)^r\right]^{1/r} \tag{28}$$

$$\sigma'_{N_1} = \sigma^0_{N_1} Q(h)\left[1+\left(\frac{l_f h}{l^2}\right)^r\right]^{-1/r} \tag{29}$$

$$\sigma_{N_2} = \sigma^0_{N_2} Q(h)\left[1+\left(\frac{e^{\pi/4}h}{3l}\right)^r\right]^{1/r} \tag{30}$$

$$\sigma'_{N_2} = \sigma^0_{N_2} Q(h)\left[1+\left(\frac{0.7470 l_f}{l^2}\right)^r\right]^{-1/r} \tag{31}$$

where r is a positive empirical constant (probably close to 1, based on analogy with other quasi-brittle materials; Bažant and Novák 2000b), and $\sigma^0_{N_1}$ and $\sigma^0_{N_2}$ are the nominal strengths corresponding to loads P_1 and P_2 calculated according to plasticity.

The overall maximum load of the floating ice always occurs for the second peak because

$$\sigma_N = \max(\sigma_{N_1}, \sigma_{N_2}) = \sigma_{N_2} \tag{32}$$

However, if the trough σ'_{N_1} is considerably smaller than σ_{N_1}, then one must design against the first peak. This means that there exists a certain critical ice thickness h^* at which the design size effect curve should jump from the σ_{N_2} curve down to σ_{N_1} curve.

Numerical Example

Figs. 7 and 8 show the calculated load-deflection curve and size effect curves for the following typical characteristics of sea ice have been assumed: $\rho = 9.81\times 10^3$ N/m^3; tensile strength $f'_t = 0.2$ MPa; fracture toughness $K_c = 0.1$ MPa $\sqrt{\text{m}}$; Poisson's ratio $\nu = 0.29$; Young's modulus $E = 1.0$ GPa; tensile strength σ_0

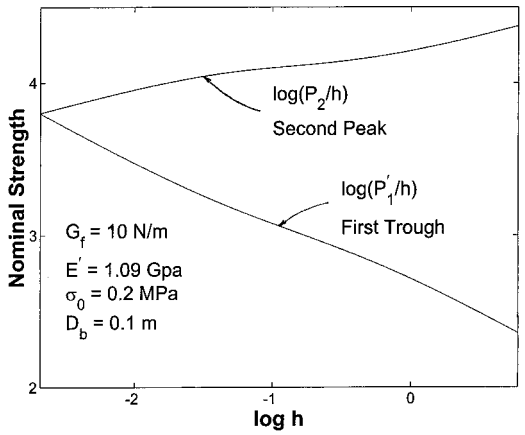

Fig. 8. Size effect obtained in numerical example

$=0.2$ MPa, with the corresponding values: fracture energy $G_f = K_c^2/E = 10$ J/m^2, and Irwin's fracture characteristic length $l_0 = (K_c/f_t')^2 = 0.25$ m.

Note that the plasticity solution, with no peaks and no size effect, applies only for ice thickness less than a few millimeters. Peaks followed by softening occur for ice thicker than about 5 cm, and peaks followed by snapback instability for ice thicker than about 20 cm about 0.1–6 m; the plots for smaller thicknesses are shown to illustrate the theory. Although the range of practical interest for the Arctic is from about 0.1 m to about 6 m, the smaller thicknesses are included in the plots in order to illustrate the theory. Obviously, the plastic response, with no size effect, is far below the practical range.

Summary and Conclusions

1. The moment-rotation diagram of the inelastic hinges in sea ice plates must exhibit postpeak softening. For the sake of simplicity, the softening is here simplified as linear. According to the energetic concept of fracture mechanics, the softening slope of the dimensionless moment-rotation diagram must get steeper as the plate thickness h increases (while in plasticity, this slope remains the same).
2. The first line hinge occurs under the load. A symmetric pair of hinges forms second in the negative moment region near the load. A further distinct symmetric pair of hinges cannot occur. Rather, the hinge region of the second-formed hinges spreads continuously toward the load. But failure must occur once a through-crack develops in the second-formed hinges.
3. For large enough h, the hinges (on one side of the load) do not soften simultaneously and the load-deflection diagram has multiple peaks and troughs; it consists of a series of spikes, which get progressively narrower as h is increased. This case is easy to solve analytically (whether or not this kind of behavior occurs for real ice thicknesses is irrelevant; the only purpose of solving this simple asymptotic case is to obtain a support for an asymptotic matching formula applicable through the entire range).
4. For the middle size range with not too large h and nonvanishing h, the hinges soften simultaneously, and there may be only one peak and no troughs. In this case, the analytical solution is complicated and an accurate solution calls for a numerical approach.
5. For vanishing h, the plasticity solution, which is also easy to obtain, must be asymptotically approached. The limit load of a plastic (shear-transmitting) floating plate under line load is unbounded unless water can flood the top of ice (the same must hold for the case of concentrated load). The reason is that the foundation provided by water buoyancy is always linear, i.e., behaves elastically.
6. There are two kinds of size effect: (a) the size effect due to formation of a finite fracture process zone at crack initiation from the surface, and (b) the size effect due to energy release as the crack in the hinge gets deep. In terms of the dimensionless nominal strength, the former size effect results in an up-and-down logarithmic size effect plot; it causes the nominal stress for each load peak to first decrease with h and then asymptotically approach for large h a rising asymptote (reverse size effect) proportional to $h^{1/4}$. The latter size effect, on the other hand, is a strong monotonic size effect; it causes the nominal strength for each trough between two spikes to decrease asymptotically as $h^{-1/2}$.
7. Compared to the case of beam structures studied separately (Bažant 2000a), the existence of the reverse size effect for the peaks at large h, and of the milder size effect for the troughs, are the consequence of buoyancy, which never ceases to grow linearly with deflection (unless water can flood the top of ice plate).
8. To obtain approximate formulas for the size effect through the entire size range, including the middle range with hinges softening simultaneously, the technique of asymptotic matching is invoked. Approximate formulas of general validity are constructed as smooth formulas whose asymptotes for large and small thickness match the exact size effect solutions for the asymptotic cases.
9. For typical sea ice properties, the hinges do not soften simultaneously and the response is very brittle, with the load-deflection diagram consisting of sharp peaks. Plastic behavior is reached only for ice thicknesses much below the range of interest.

Acknowledgments

Partial financial support has been received under Grant No. N00014-91-J-1109 from the Office of Naval Research and Grant No. CMS-9713944 from the National Science Foundation, both to Northwestern University.

Appendix: Combined Energetic-Statistical Size Effect

The entire present analysis can be easily generalized to include the Weibull-type statistical size effect on the mean strength (Bažant and Planas 1998, Chap. 12; Bažant and Novák 2000b). It would suffice to replace function $Q(h)$ defined by Eq. (1) with the formula

$$\frac{1}{Q(h)} = \left[\left(\frac{D_b}{\eta D_b + h} \right)^{rn/m} + \frac{rD_b}{\eta D_b + h} \right]^{1/r} \tag{33}$$

(Bažant 2001c) where n = Weibull modulus (typically 20–50); $n_d = 2$ = number of spatial dimensions; and r, η = constants (r is usually close to 1). Since normally $rn_d/n \ll 1$, this formula deviates significantly from the definition of $Q(h)$ in Eq. (1) only for $h \gg D_b$.

References

Barenblatt, G. I. (1979). *Similarity, self-similarity and intermediate asymptotics*, Consultants Bureau, New York.

Bažant, Z. P. (1984). ''Size effect in blunt fracture: concrete, rock, and metal.'' *J. Eng. Mech.*, 110(4), 518–535.
Bažant, Z. P. (1992a). ''Large-scale thermal bending fracture of sea ice plates.'' *J. Geophys. Res., C: Oceans Atmos.*, 97(C11), 17739–17751.
Bažant, Z. P. (1992b). ''Large-scale fracture of sea ice plates.'' *Proc., 11th IAHR Ice Symposium, Banff, Alberta*, June, T. M. Hrudey, ed., Dept. of Civil Engineering, Univ. of Alberta, Edmonton, Vol. 2., 991–1005.
Bazant, Z. P. (1993). ''Scaling laws in mechanics of failure.'' *J. Eng. Mech.*, 119(9), 1828–1844.
Bazant, Z. P. (1997). ''Scaling of quasibrittle fracture: Asymptotic analysis.'' *Int. J. Fract.*, 83(1), 41–65.
Bažant, Z. P. (1999). ''Size effect on structural strength: a review.'' *Archives of applied mechanics*, Vol. 69, Ingenieur-Archiv, Springer, Berlin, 703–725.
Bažant, Z. P. (2000a). ''Asymptotic matching analysis of scaling of structural failure due to softening hinges.'' *Structural Engineering Rep. No. 00-11/C402s*, Northwestern Univ., Evanston, IL.
Bažant, Z. P. (2000b). ''Scaling laws for brittle failure of sea ice.'' *Preprints, IUTAM Symp., Scaling Laws in Ice Mechanics*, Univ. of Alaska, Fairbanks, June, J. P. Dempsey, H. H. Shen, and L. H. Shapiro, eds., Paper No. 3, 1–23.
Bažant, Z. P. (2001a). ''Scaling laws for sea ice fracture.'' *Scaling Laws in Ice Mechanics (Proc., IUTAM Symp., Fairbanks 2000)*, J. P. Dempsey et al., eds. (in press).
Bažant, Z. P. (2001b). ''Size effects in quasibrittle fracture: Apercu of recent results.'' *Fracture Mechanics of Concrete Structures (Proc., FraMCoS-4 Int. Conf., Paris)*, R. de Borst et al., eds., Swets and Zeitlinger, Balkema, Lisse, 651–658.
Bažant, Z. P. (2002). *Size effect on structural strength*, Hermes Scientific, Oxford–Paris.
Bažant, Z. P., and Cedolin, L. (1991). *Stability of structures: elastic, inelastic, fracture and damage theories*, Oxford University Press, New York.
Bažant, Z. P., and Chen, E.-P. (1997). ''Scaling of structural failure.'' *Appl. Mech. Rev.*, 50(10), 593–627.
Bažant, Z. P., and Gettu, R. (1991). ''Size effects in the fracture of quasibrittle materials.'' *Cold Regions Engineering (Proc., 6th ASCE International Specialty Conf.*, Hanover, N.H., Feb. 1991), D. S. Sodhi, ed., ASCE, New York, 595–604.
Bažant, Z. P., and Kim, Jenn-Keun. (1985). ''Fracture theory for nonhomogeneous brittle materials with application to ice.'' *Proc., ASCE Nat. Conf. on Civil Engineering in the Arctic Offshore—ARCTIC 85*, San Francisco, L. F. Bennett, ed., ASCE, New York, 917–930.
Bažant, Z. P., and Kim, H. Jang-Jay. (1998a). ''Size effect in penetration of sea ice plate with part-through cracks. I. Theory.'' *J. Eng. Mech.*, 124(12), 1310–1315.
Bažant, Z. P., and Kim, H. Jang-Jay. (1998b). ''Size effect in penetration of sea ice plate with part-through cracks. II. Results.'' *J. Eng. Mech.*, 124(12), 1316–1324.
Bažant, Z. P., and Kim, H. Jang-Jay. (2000). ''Closure of Discussion on 'Size effect in penetration of sea ice plate with part-through cracks. I. Theory, and II. Results'. '' *J. Eng. Mech.*, 126(4), 440–442.
Bažant, Z. P., Kim, Jang-Jay H., and Li, Y.-N. (1995). ''Part-through bending cracks in sea ice plates: Mathematical modeling.'' *ICE MECHANICS-1995*, J. P. Dempsey and Y. Rajapakse, eds., Vol. 207, 97–105.
Bažant, Z. P., and Li, Y.-N. (1994). ''Penetration fracture of sea ice plate: Simplified analysis and size effect.'' *J. Eng. Mech.*, 120(6), 1304–1321.
Bažant, Z. P., and Li, Y.-N. (1995a). ''Penetration fracture of sea ice plate.'' *Int. J. Solids Struct.*, 32, 3/4, 303–313.
Bažant, Z. P., and Li, Z. (1995b). ''Modulus of rupture: size effect due to fracture initiation in boundary layer.'' *J. Struct. Eng.*, 121(4), 739–746.
Bažant, Z. P., and Li, Z. (1996). ''Zero-brittleness size-effect method for one-size fracture test of concrete.'' *J. Eng. Mech.*, 122(5), 458–468.
Bažant, Z. P., and Novák, D. (2000a). ''Probabilistic nonlocal theory for quasibrittle fracture initiation and size effect. I. Theory. II. Application.'' *J. Eng. Mech.*, 126(2), 166–174 and 175–185.
Bažant, Z. P., and Novák, D. (2000b). ''Energetic-statistical size effect in quasibrittle failure at crack initiation.'' *ACI Mater. J.*, 97(3), 381–392.
Bažant, Z. P., and Planas, J. (1998). *Fracture and size effect in concrete and other quasibrittle materials*, CRC, Boca Raton, Fla.
Bender, M. C., and Orszag, S. A. (1978). *Advanced mathematical methods for scientists and engineers*, McGraw–Hill, New-York, Chap. 9–11.
Bernstein, S. (1929). *The railway ice crossing (in Russian), Trudy Nauchno-Technicheskogo Komiteta Narodnogo Komissariata Putei, Soobshchenniya*, Vol. 84, Moscow.
Butiagin, I. P. (1966). *Strength of ice and ice cover*, Izdatel'stvo Nauka, Sibirskoe Otdelenie, Novosibirsk, Russia, 154.
Dempsey, J. P. (1991). ''The fracture toughness of ice.'' *Ice Structure Interaction*, S. J. Jones, R. F. McKenna, J. Tilotson, and I. J. Jordaan, eds., Springer, Berlin, 109–145.
Dempsey, P. P. (2000). ''Discussion of 'Size effect in penetration of ice plate with part-through cracks. I. Theory, II. Results.' by Z. P. Bažant, and J.-J. H. Kim.'' *J. Eng. Mech.*, 126(4), 438.
Dempsey, J. P., Adamson, R. M., and Mulmule, S. V. (1995), ''Large-scale in-situ fracture of ice.'' *Proc., FRAMCOS-2*, F. H. Wittmann, ed., *AEDIFICATIO*, D-79104 Freiburg, 1995.
Dempsey, J. P., DeFranco, S. J., Adamson, R. M., and Mulmule, S. V. (1999a). ''Scale effects on the *in situ* tensile strength and fracture of ice: Part I.: Large grained freshwater ice at Spray Lakes Reservoir, Alberta.'' *Int. J. Fract.*, 95(1999), 325–345.
Dempsey, J. P., Adamson, R. M., and Mulmule, S. V. (1999b). ''Scale effects on the *in situ* tensile strength and fracture of ice: Part II.: First-year sea ice at Resolute, N.W.T.'' *Int. J. Fract.*, 95, 346–378.
Dempsey, J. P., Slepyan, L. I., and Shekhtman, I. I. (1995). ''Radial cracking with closure.'' *Int. J. Fract.*, 73(3), 233–261.
DeFranco, S. J., and Dempsey, J. P. (1992). ''Nonlinear fracture analysis of saline ice: Size, rate and temperature effects.'' *Proc., 11th IAHR Symposium*, Banff, Alberta, Vol. 3, 1420–1435.
DeFranco, S. J., and Dempsey, J. P. (1994). ''Crack propagation and fracture resistance in saline ice.'' *J. Glaciol.*, 40, 451–462.
DeFranco, S. J., Wei, Y., and Dempsey, J. P. (1991). ''Notch acuity effects on fracture of saline ice.'' *Ann. Glaciol.*, 15, 230–235.
Epstein, B. (1948). ''Statistical aspects of fracture problems.'' *J. Appl. Phys.*, 19, 140–147.
Fisher, R. A., and Tippett, L. H. C. (1928). ''Limiting forms of the frequency distribution of the largest and smallest member of a sample.'' *Proc. Cambridge Philosophical Soc.*, 24, 180–190.
Frankenstein, E. G. (1963). ''Load test data for lake ice sheet.'' *Technical Rep. No. 89*, U.S. Army Cold Regions Research and Engineering Laboratory, Hanover, N.H.
Frankenstein, E. G. (1966). ''Strength of ice sheets.'' *Proc., Conf. on Ice Pressures against Struct. Tech. Memor. No. 92, NRCC No. 9851*, Laval Univ., Quebec, National Research Council of Canada, Canada, 79–87.
Frechet, M. (1927). ''Sur la loi de probabilite de l'ecart maximum.'' *Ann. Soc. Polon. Math.*, 6, 93.
Freudenthal, A. M., and Gumbel, E. J. (1956). ''Physical and statistical aspects of fracture.'' *Advances in applied mechanics*, Academic, Vol. 4, 117–157.
Gumbel, E. J. (1958). *Statistics of extremes*, Columbia University Press, New York.
Hinch, E. J. (1991). *Perturbation Methods*, Cambridge University Press, Cambridge, U.K.
Jirásek, M., and Bažant, Z. P. (2002). *Inelastic analysis of structures*, Wiley, London.
Kerr, A. D. (1975). ''The bearing capacity of floating ice plates subjected to static or quasi-static loads—A critical survey.'' *Research Rep. No. 333*, U.S. Army Cold Regions Research and Engineering Laboratory, Hanover, N.H.
Kerr, A. D. (1996), ''Bearing capacity of floating ice covers subjected to static, moving, and oscillatory loads.'' *Appl. Mech. Rev., reprint*, 49(11), 463–476.
Kittl, P., and Diaz, G. (1988). ''Weibull's fracture statistics, or probabi-

listic strength of materials: state of the art.'' *Res. Mech.*, 24, 99–207.
Li, Y.-N., and Bažant, Z. P. (1994). ''Penetration fracture of ice plate: 2D analysis and size effect.'' *J. Eng. Mech.*, 120(7), 1481–1498.
Li, Zhengzhi, and Bažant, Z. P. (1998). ''Acoustic emissions in fracturing sea ice plate simulated by particle system.'' *J. Eng. Mech.*, 124(1), 69–79.
Lichtenberger, G. J., Jones, J. W., Stegall, R. D., and Zadow, D. W. (1974). ''Static ice loading tests Resolute Bay—Winter 1973/74.'' *APOA Proj. No. 64, Rep. No. 745B-74-14*, (CREEL Bib No. 34-3095), Sunoco Sci. & Technol., Rechardson, Tex.
Mariotte, E. (1686). *Traité du mouvement des eaux*, posthumously edited by M. de la Hire, English translation by J. T. Desvaguliers, London (1718), 249; also *Mariotte's collected works*, 2nd Ed., The Hague (1740).
von Mises, R. (1936). ''La distribution de la plus grande de n valeurs.'' *Revue mathématique de l'Union interbalcanique* (Athens), Vol. 1, No. 1.
Mulmule, S. V., Dempsey, J. P., and Adamson, R. M. (1995). ''Large-scale in-situ ice fracture experiments—part II: modeling efforts, in ice mechanics—1995.'' *ASME Joint Applied Mechanics and Materials Summer Conf.*, AMD-MD, Univ. California, Los Angeles, June 28–30.
Nevel, D. E. (1958). ''The theory of narrow infinite wedge on an elastic foundation.'' *Trans. Eng. Institute Canada*, 2(3).
Peirce, F. T. (1926). ''Tensiletests of cotton yarns: V. The weakest link.'' *J. Text. Inst.*, 17, 355–368.
Rice, J. R., and Levy, N. (1972). ''The part-through surface crack in an elastic plate.'' *J. Appl. Mech.*, 39, 185–194.
Sanderson, T. J. O. (1988). *Ice mechanics: Risks to offshore structures*, Graham and Trotman, London.
Schulson, E. M. (1990). ''The brittle compressive fracture of ice.'' *Acta Metall. Mater.*, 38(10), 1963–1976.
Schulson, E. M. (2001). ''Brittle failure of ice.'' *Eng. Fract. Mech.*, 68(17–18), 1839–1887.
Sedov, L. I. (1959). *Similarity and dimensional methods in mechanics*, Academic, New York.
Slepyan, L. I. (1990). ''Modeling of fracture of sheet ice,'' *Mech. Solids, (transl. of Izv. AN SSSR Mekhanika Tverdoga Tela)*, 25(2), 155–161.
Sodhi, D. S. (1995a). ''Breakthrough loads of floating ice sheets.'' *J. Cold Reg. Eng.*, 1, 4–20.
Sodhi, D. S. (1995b). ''Wedging action during vertical penetration of floating ice sheets.'' *Ice mechanics*, AMD Vol. 207, No. H00954, 65–80.
Sodhi, D. S. (1996). ''Deflection analysis of radially cracked floating ice sheets.'' *Proc., 17th Int. Conf. OMAE*, No. G00954, 97–101.
Sodhi, D. S. (1998). ''Vertical penetration of floating ice sheets.'' *Int. J. Solids Struct.*, 35(31–32), 4275–4294.
Sodhi, D. S. (2000). ''Discussion of 'Size effect in penetration of ice plate with part-through cracks. I: Theory; II: Results' by Z. P. Bažant and J. J. H. Kim.'' *J. Eng. Mech.*, 126(4), 438–440.
Tippett, L. H. C. (1925). ''On the extreme individuals and the range of samples.'' *Biometrika*, 17, 364.
Weeks, W. F., and Assur, A. (1972). ''Fracture of lake and sea ice.'' *Fracture*, H. Liebowitz, ed., Vol. II, 879–978.
Weeks, W. F., and Mellor, M. (1984). ''Mechanical properties of ice in the Arctic seas.'' *Arctic technology and policy*, I. Dyer and C. Chryssostomidis, eds., Hemisphere, Washington, D.C., 235–259.
Weibull, W. (1939). ''The phenomenon of rupture in solids.'' *Proc., Royal Swedish Institute Engineering Research (Ingenioersvetenskaps Akad. Handl.)*, Vol. 153, Stockholm, 1–55.
Weibull, W. (1951). ''A statistical distribution function of wide applicability.'' *J. Appl. Mech.*, 18, 293–297.